UC Irvine
UC Irvine Previously Published Works

Title

Characterization of the Temporomandibular Joint Disc Complex in the Yucatan Minipig

Permalink

https://escholarship.org/uc/item/6qk8p0b3

Journal

Tissue Engineering Part A, 29(15-16)

ISSN

1937-3341

Authors

Donahue, Ryan P

Kallins, Eston G

Hu, Jerry C

et al.

Publication Date

2023-08-01

DOI

10.1089/ten.tea.2023.0011

Peer reviewed

termis.

Tissue Engineering
& Regenerative Medicine
International Society

Open camera or QR reader and
scan code to access this article
and other resources online.

ORIGINAL ARTICLE

Characterization of the Temporomandibular Joint Disc Complex in the Yucatan Minipig

Ryan P. Donahue, PhD,* Eston G. Kallins,* Jerry C. Hu, PhD, and Kyriacos A. Athanasiou, PhD

The temporomandibular joint (TMJ) disc complex (i.e., the TMJ disc and its six attachments) is crucial to everyday functions such as mastication and speaking. The TMJ can be afflicted by many conditions, including disc displacement and defects. Pathologies of the TMJ disc complex most commonly present first as anterior disc displacement, which the field hypothesizes may implicate the two posterior attachments. As a result of anterior disc displacement, defects may develop in the lateral disc complex. Tissue engineering is poised to improve treatment paradigms for these indications of the TMJ disc complex by engineering biomimetic implants, but, first, gold-standard design criteria for such implants should be established through characterization studies. This study's objective was to characterize the structural, mechanical, biochemical, and crosslinking differences among the two posterior attachments and the lateral disc in the Yucatan minipig, a well-accepted TMJ animal model. In tension, it was found that the posterior inferior attachment (PIA) was significantly stiffer and stronger by 2.13 and 2.30 times, respectively, than the posterior superior attachment (PSA). It was found that collagen in both attachments was primarily aligned mediolaterally; however, the lateral disc was much more aligned and anisotropic than either attachment. Among the three locations, the PSA exhibited the greatest degree of heterogeneity and highest proportion of fat vacuoles. The PIA and lateral disc were 1.93 and 1.91 times more collagenous, respectively, by dry weight (DW) than the PSA. The PIA also exhibited 1.78 times higher crosslinking per DW than the PSA. Glycosaminoglycan per DW was significantly higher in the lateral disc by 1.48 and 5.39 times than the PIA and PSA, respectively. Together, these results establish design criteria for tissue-engineering of the TMJ disc complex and indicate that the attachments are less fibrocartilaginous than the disc, while still significantly contributing to the mechanical stability of the TMJ disc complex during articulation. These results also support the biomechanical function of the PIA and PSA, suggesting that the stiffer PIA anchors the disc to the mandibular condyle during articulation, while the softer PSA serves to allow translation over the articular eminence.

Keywords: TMJ disc complex, TMJ disc, TMJ disc attachments, characterization, tissue engineering

Impact Statement

Characterization of the temporomandibular joint (TMJ) disc complex (i.e., the disc and its attachments) has important implications for those aiming to tissue-engineer functional replacements and can help elucidate its biomechanical function. For example, the findings shown here suggest that the stiffer posterior inferior attachment anchors the disc during articulation, while the softer posterior superior attachment allows translation over the articular eminence.

Department of Biomedical Engineering, University of California, Irvine, Irvine, California, USA.
*These authors contributed equally to this article.

Introduction

THE TEMPOROMANDIBULAR JOINT (TMJ) is a ginglymo-arthrodial joint responsible for mastication and speaking.[1] Central to the function of the TMJ is the articulation of the TMJ disc between the mandibular condyle and mandibular fossa/articular eminence (Fig. 1).[2] During articulation, the TMJ disc is held in position by six attachments, which surround the entire periphery of the disc. The anterior and posterior regions of the disc are each connected by two attachments that split into superior and inferior directions so as to attach the disc to the skull and mandibular condyle, while the sides of the disc are attached to the mandibular condyle through the lateral and medial attachments (Fig. 1).[3] Together, these structures, termed the TMJ disc complex, allow for smooth articulation during the intricate rotational and translational movement of the joint and are subjected to a combination of tensile, compressive, and shear stresses during articulation.[4] Excessive or abnormal loading of the TMJ disc complex due to trauma and/or age-related deterioration can occur, often leading to temporomandibular disorders (TMDs).

An estimated 5–25% of the population is affected by the various symptoms associated with the ''TMD'' umbrella of conditions.[5–9] Specifically, a condition known as disc displacement occurs in up to 70% of cases.[10] More specifically, disc displacement occurs most frequently in the anterior direction.[11–13] It has been hypothesized in the TMJ field that the prevalence of displacement in the anterior direction strongly implicates the two posterior attachments in potential pathological progression.[14] Furthermore, these pathologies can result in eventual defects such as tissue thinning as well as complete perforation in 10–15% of disc displacement cases.[15–17] For example, in a study that examined anterior disc displacement and subsequent defect location, a majority (53.7%) of cases developed a defect in the lateral third of the disc after anterior disc displacement.[18] While anterior disc displacement and lateral defects of the TMJ disc complex are significant clinical indications, current treatments for these conditions are inadequate, as reviewed elsewhere.[4,19–21] There is a need in the TMJ field for further development of regenerative solutions for TMJ afflictions.[19]

Toward tissue-engineering of the TMJ disc complex, previous characterization studies of the TMJ disc specify this tissue's design criteria, which are the desirable objectives in terms of structural, mechanical, and biochemical properties that one aims for when producing biomimetic implants. For example, in Yucatan minipigs, the structure of the central region of the TMJ disc is anteroposterior (AP) collagen alignment. This alignment manifests in stiffness and strength values being 17.2 and 17.1 times higher, respectively, in the AP direction, compared with the medio-lateral (ML) direction.[22] This is analogous to the central portion of the human TMJ disc, which has been shown to have collagen alignment in the AP direction as well.[23] Additional characterizations have shown that the TMJ disc is understood to function as a trampoline-like structure,[24] being 100 to 1000 times stiffer in tension than compression.[25] However, the posterior attachments are far less characterized. While such studies exploring the posterior attachments are limited in number, previous literature in juvenile porcine samples has shown that the posterior inferior attachment (PIA) is 5.0 times stiffer and 3.0 times stronger in the AP direction compared with the posterior superior attachment (PSA),[26] which supports their respective roles; the PIA maintains disc positioning on top of the condyle, while the PSA allows the translational movement of the joint.[26] Due to the implicated role of the two posterior attachments in anterior disc displacement, the TMJ field will directly benefit from defining design criteria for tissue-engineering toward regeneration of the TMJ disc complex as a whole.

To further understand the structure and function of the TMJ disc complex, specifically, the posterior attachments, tissue engineers frequently use animal models, such as goats, sheep, pigs, and minipigs,[27] to model the human condition. For example, extensive characterization of the Yucatan minipig's TMJ[22] has demonstrated its similarities to human TMJs, making it an ideal model for additional characterizations and for testing tissue-engineered therapeutics.[28] Thus, this study aims to characterize the differences among the PIA, PSA, and lateral disc in skeletally mature Yucatan minipigs to further develop design criteria for tissue engineers. The lateral disc was also characterized in this study due to its established structure–function relationships and

FIG. 1. Anatomy of the TMJ disc complex. The TMJ is found between the base of the skull and the mandible (sagittal view). More specifically, the TMJ disc complex is situated between the mandibular condyle and mandibular fossa/articular eminence. The TMJ disc complex is made up of the TMJ disc and its six attachments. The posterior and anterior attachments split superiorly and inferiorly to attach to the skull and mandibular condyle, respectively, while the lateral and medial attachments connect inferiorly to the mandibular condyle. TMJ, temporomandibular joint. Color images are available online.
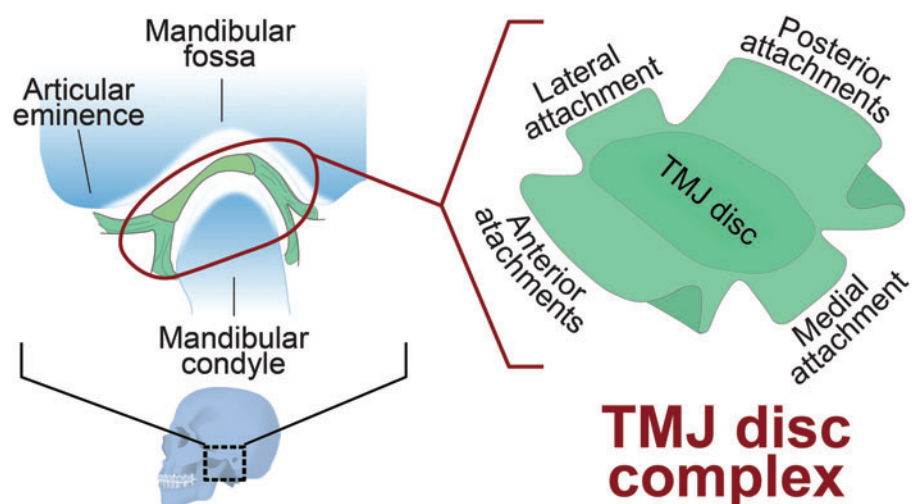
the propensity for defects to develop in this region as a result of anterior disc displacement. Due to inherent differences in function between the posterior attachments and the TMJ disc, it was hypothesized that there will be significant organizational, mechanical, biochemical, and cross-linking differences among the PIA, PSA, and lateral disc.

Materials and Methods

Tissue procurement

TMJ disc and posterior attachment samples were obtained from eight (*n* = 4 castrated males and *n* = 4 intact females) skeletally mature (18–24 months old) Yucatan minipigs (*Sus scrofa domesticus*) that were culled for purposes unrelated to this study. In terms of distribution, five samples (*n* = 3 males and *n* = 2 females) and three samples (*n* = 1 male and *n* = 2 females) were sourced from Premier BioSource and Lonestar Laboratory Swine, respectively, resulting in an equal proportion of males and females in this study in accordance with the National Institutes of Health (NIH) policy on sex as a biological variable.[29] The sample number was based on power analysis of tensile testing outcomes from prior studies. Up to five freeze–thaw cycles have been shown to not affect material properties of the porcine TMJ disc.[30] However, joints were fresh-frozen whole only once before tissue dissection. Upon thawing, the TMJ was approached through the skin, fat, muscle, and periosteum, taking care not to damage tissue structures of interest. Briefly, the superior joint space was breached through sharp dissection, cutting along the perimeter of the superior disc surface and joint capsule elements to detach the disc and posterior attachments from the mandibular fossa and articular eminence. The condylar head was freed from the ramus by use of an oscillating saw to cut through the condylar neck. The TMJ disc and posterior attachments were then freed from the condylar head by sharp dissection around the perimeter of the inferior surface of the disc and joint capsule elements. This left the TMJ disc with the posterior attachments remaining, from which samples were obtained for histology and polarized light microscopy, mechanical testing, photometric biochemical assays, and mass spectrometry crosslinks assay (Fig. 2). From each animal, one disc complex was used for ML mechanical testing and histology, while the other disc complex was used for AP mechanical testing, photometric biochemistry assays, and mass spectrometry crosslinks analysis (Fig. 2). To ensure equal variance between right and left joints, the samples were gathered from alternating sides from one animal to the next.

Histology and polarized light microscopy

Samples were obtained for histological stains, including hematoxylin and eosin (H&E), picrosirius red, and safranin O with fast green counterstain, as previously reported.[31] Briefly, biopsy punches of 3 mm diameter (dia.) were taken from the full-thickness samples of the tissue (Fig. 2). Then, the cylindrical tissues were sectioned transversely; fixed in 10% neutral-buffered formalin; processed using a standard series of dehydration, clearing, and paraffin infiltration steps; embedded in paraffin; sectioned at 5 μm; and mounted on slides before staining. Slides were subsequently stained using H&E, picrosirius red, and safranin O with fast green and imaged using a bright-field microscope. Additionally, picrosirius red-stained samples were subjected to polarized light microscopy to observe collagen alignment under a polarizer.[32]

Mechanical testing

Uniaxial mechanical testing was performed for excised samples of the TMJ disc complex in the AP and ML directions (Fig. 2). Briefly, samples were clamped using hemostats attached to a uniaxial testing machine (Instron 5655). Samples were subjected to a tare load of 0.2 N to remove excess slack from the samples. The gauge length was
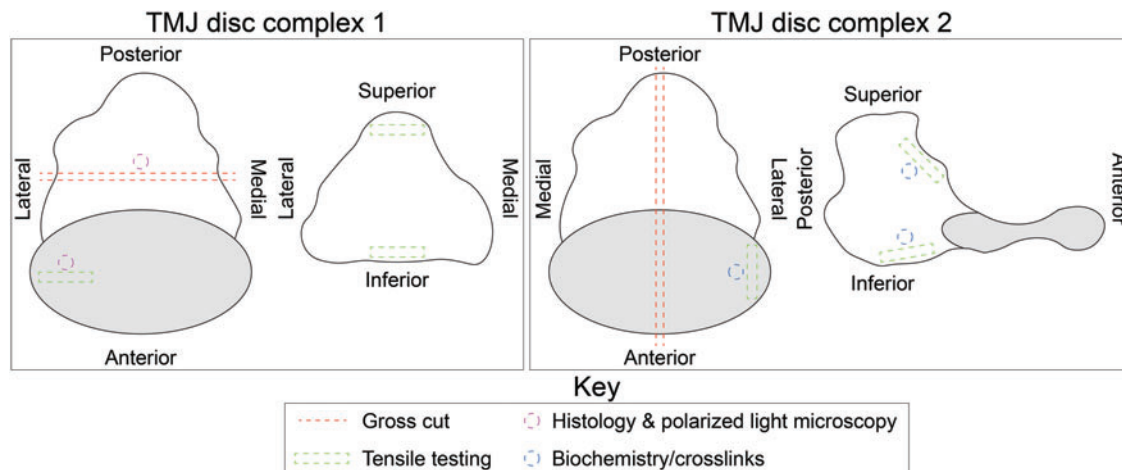

FIG. 2. Sample collection from the TMJ disc complex. From each animal, two TMJ disc complexes were collected, which were grossly cut sagittally or coronally (*red* dashed lines) to obtain samples for testing. Samples for histology and polarized light microscopy were collected using a 3 mm diameter biopsy punch (*pink* dashed circles). Tensile testing samples were cut as rectangular wedges of tissue (*green* dashed rectangles), while biochemistry/crosslink samples were collected using a 3 mm diameter biopsy punch (*blue* dashed circles). TMJ, temporomandibular joint. Color images are available online.

measured as the tip-to-tip length between the hemostats (4.708 ± 2.351 mm), and images were taken before the start of the uniaxial tensile test for measurement of the initial cross-sectional area (4.229 ± 1.896 mm^2). Samples were then pulled at a rate of 1% strain per second until complete failure. Samples that failed near the hemostats were excluded from the data and were rerun with new tissue samples. Of 48 total uniaxial testing samples, only two broke close to the clamps; for these two, adjacent samples were excised and tested again. Resulting force–displacement curves were analyzed using a custom MATLAB script to convert the data to stress–strain curves and determine Young's modulus, ultimate tensile strength (UTS), strain at failure, toughness (energy absorbed to complete failure, i.e., the entire area under the stress–strain curve), and resilience (energy absorbed in the elastic region, i.e., the area under the curve of the linear region of the stress–strain curve) of the samples. Throughout the text, we use "stiffer," "softer," "stronger," and "weaker" to denote a sample that has a higher Young's modulus, lower Young's modulus, higher UTS, and lower UTS, respectively.

Photometric biochemical assays

Excised samples (~ 3 mm dia. biopsy punch) were weighed while hydrated, placed on a lyophilizer, and weighed again after drying. Hydration was calculated as the difference between the sample wet weight (WW) and dry weight (DW) divided by the original WW and expressed as a percentage. As previously described, total collagen content was measured using a modified hydroxyproline assay,[33] while sulfated glycosaminoglycan (GAG) content was measured using a dimethylmethylene blue assay according to the manufacturer's instructions. Samples were then normalized to WW and DW. Three technical replicates per biological sample were run and averaged for each assay to obtain a singular measurement.

Mass spectrometry crosslinks assay

Quantification of pyridinoline (PYR) crosslinks was performed through mass spectrometry, as previously reported.[34] Briefly, excised samples of about 1 mg in WW (from the same tissue as biochemical samples) were lyophilized, weighed again to obtain the DW, washed in ultrapure water overnight on a shaker, and hydrolyzed overnight in 4 N HCl. Hydrolysates were then resuspended, filtered using a 100-kDa cutoff filter, and diluted (1:10) before being subjected to liquid chromatography–mass spectrometry with a Waters ACQUITY QDa. PYR standards were used to quantify the molecule in each sample, and the molecule was normalized to WW, DW, and total collagen (from the hydroxyproline assay).

Statistical analyses

Mechanical testing outcomes were analyzed using a two-way analysis of variance (ANOVA) with testing direction and location as the two factors. Bonferroni's *post hoc* test was used to compare the testing direction within each location (depicted with asterisks). Tukey's *post hoc* test was used to compare among locations with values aggregated from both testing directions (depicted with Latin letters through a connecting letters report in the X-axis labels; groups that share a letter are not statistically significant). Biochemical and crosslink outcomes were analyzed using a one-way ANOVA with Tukey's *post hoc* test (depicted with Latin letters through a connecting letters report). An *a posteriori* statistical analysis showed animal sex was not a significant factor in any outcome measure. Pearson's correlations were run to identify correlations between mechanical properties and biochemical properties (including crosslinking outcomes) to identify potential structure–function relationships. Significant correlations and the coefficient of determination (r^2) are reported. The threshold for statistical significance for all tests was set as $p < 0.05$. All bars are shown as mean $\pm$ standard deviation.

Results

Histology and polarized light microscopy

Histology images with H&E, picrosirius red, picrosirius red under polarized light, and safranin O with fast green staining are shown in Figure 3. The PIA exhibited a mostly dense matrix with sparse pockets of fat vacuoles (Fig. 3). The PSA samples were more heterogeneous than the PIA and lateral disc, exhibiting approximately 50% of the tissue being made up of fat vacuoles (Fig. 3). Outside of the areas containing fat vacuoles, all three tissues exhibited similar intensities of picrosirius red staining for total collagen (Fig. 3). When examining the picrosirius red staining under polarized light microscopy, the alignment of collagen of the PIA and PSA appeared predominantly in the ML direction, while the lateral disc appeared almost entirely aligned in the AP direction (Fig. 3). The tissues appeared completely devoid of GAG, as shown by the safranin O with fast green staining (Fig. 3).

Mechanical analysis

Uniaxial tensile testing outcomes are shown in Figure 4. Both Young's modulus and UTS values for the PIA tested in the ML direction were significantly higher than the AP values ($p < 0.0367$) (Fig. 4). When comparing the testing directionality using the ratio of Young's modulus values of the AP and ML directions, the PIA, PSA, and lateral disc had values of 2.78, 3.41, and 7.74, respectively; the lateral disc's ratio was at least 2.27 times that of either posterior attachment. When compared with the PSA, the PIA was also significantly 2.13 times stiffer and 2.30 times stronger ($p < 0.0371$) (Fig. 4). When examining strain at failure, there were no statistically significant findings, but the PIA strained the most in the AP direction, while the lateral disc strained most in the ML direction (Fig. 4). As for toughness and resilience, the lateral disc values were significantly higher in the AP direction compared with the ML direction ($p < 0.0017$) (Fig. 4). The lateral disc was also significantly tougher and more resilient compared with the PSA ($p < 0.0016$), while the PIA also trended higher than the PSA (Fig. 4).

Photometric biochemical analyses

Outcomes from the photometric biochemical analyses are shown in Figure 5. In terms of total collagen content per WW and DW, the PIA value was the highest (Fig. 5). The
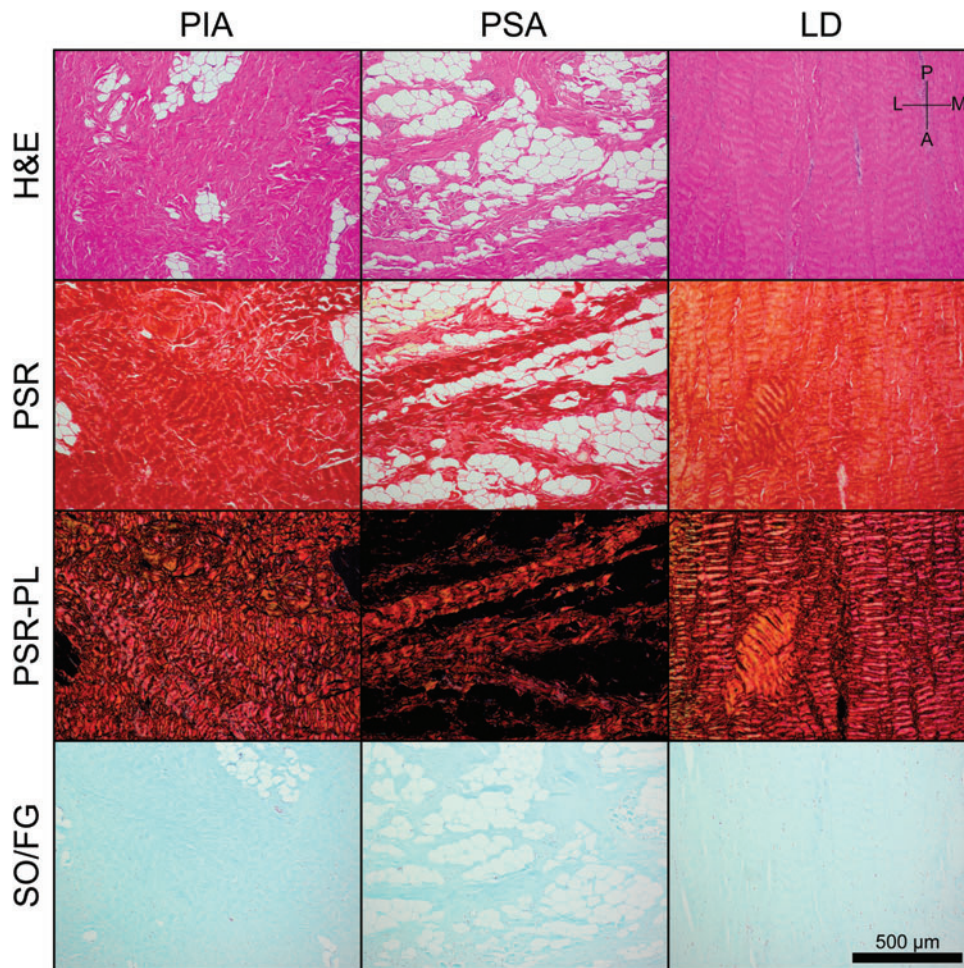
FIG. 3. Histology and polarized light microscopy of the TMJ disc complex. As shown in H&E staining, the PIA exhibits more homogeneity in matrix content similar to the lateral disc, but unlike the PSA. Both the PIA and PSA exhibit varying presence of fat vacuoles, unlike the lateral disc. Outside of the fatty areas, the tissues are all highly collagenous, as shown in the PSR. Under polarized light microscopy, PSR enhanced the birefringence of collagen fibrils and allowed visualization of the collagen fiber alignment. The PIA has mostly ML alignment along with the PSA; however, the lateral disc has almost complete AP alignment. Safranin O staining with fast green counterstain shows the extremely low GAG content of all three tissues. A, anterior; AP, anteroposterior; H&E, hematoxylin and eosin; GAG, glycosaminoglycan; L, lateral; LD, lateral disc; M, medial; ML, mediolateral; P, posterior; PIA, posterior inferior attachment; PL, polarized light; PSA, posterior superior attachment; PSR, picrosirius red; SO/FG, safranin O with fast green; TMJ, temporomandibular joint. Color images are available online.

PIA value was also higher by 1.93 times when compared with the PSA in terms of total collagen per DW ($p = 0.0002$) (Fig. 5). In terms of GAG content, the lateral disc value was significantly higher than both the PIA and PSA values ($p < 0.0368$) when normalized to both WW and DW, while the PSA value was the lowest (2.85–3.65 times lower than PIA, $p < 0.0004$) (Fig. 5). Hydration values for the PIA and lateral disc were also 1.34 and 1.38 times higher, respectively, than the PIA ($p < 0.0010$) (Fig. 5). Total collagen per DW was statistically, but weakly, correlated with UTS ($r^2 = 0.17$) and toughness ($r^2 = 0.25$) in the AP direction.

Crosslinking mass spectrometry analysis

Outcomes from the crosslinking mass spectrometry analysis are shown in Figure 6. When normalized to both WW and DW, the PIA was the most crosslinked of all locations tested (Fig. 6). For PYR per WW, the PIA value was significantly higher than the lateral disc value by 1.57 times ($p = 0.0248$) (Fig. 6), while the PIA value was significantly higher than the PSA value when normalized to DW ($p = 0.0205$) (Fig. 6). While the PYR per total collagen content was not significantly different between the locations tested, the degree of crosslinking trended higher in the PIA and PSA groups (Fig. 6). PYR per WW ($r^2 = 0.19$) and DW ($r^2 = 0.25$) values were both statistically correlated with strain at failure in the AP direction.

Discussion

The aim of this study was to characterize the PIA, PSA, and lateral disc toward identifying design criteria for tissue-engineered constructs for the TMJ disc complex. More specifically, this study used histology and polarized light microscopy, uniaxial tensile testing, photometric biochemical tests, and mass spectrometry crosslinks analysis to highlight differences among the PIA, PSA, and lateral disc. It was hypothesized that there would be variations in organization, mechanical properties, biochemical properties, and crosslinking content of the PIA, PSA, and lateral disc. The hypothesis was confirmed. Specifically, the PIA was stiffer and stronger than PSA; these observations were supported by collagen and crosslinking data for the posterior attachments. For example, the PYR crosslinking content in the PIA was higher than that of the PSA. Both attachments also exhibited more heterogeneous matrices; whereas the lateral disc exhibited a fibrous matrix, the attachments contained regions with fat vacuoles. In addition, the attachments contained less GAG content than the fibrocartilaginous lateral disc. Although the attachments did not display histological similarities to ligaments, the mechanical properties supported the notion that the attachments serve a ligament-like role during articulation with the joint. Specifically, the stiffer PIA may serve a critical role in securing the disc to the condyle and protecting the disc from anterior disc displacement, while the softer PSA may

FIG. 4. Uniaxial tensile testing outcomes of the TMJ disc complex. When examining Young's modulus and UTS, both the PIA and lateral disc exhibit significant differences when comparing testing directions, denoting significant anisotropy. The PSA was less stiff and weaker than the PIA and lateral disc in both cases. Strain at failure did not differ between samples. For toughness and resilience, the lateral disc values were higher than the PSA in both outcomes, while the PIA also trended higher than the PSA. Statistics: two-way ANOVA, $p < 0.05$. Bonferroni's *post hoc* test between the outcomes of the testing directions within each location is depicted by an *asterisk* (*). Tukey's *post hoc* test among the locations with values aggregated from both testing directions is depicted with Latin letters in the X-axis labels using a connecting letters report (groups that share a letter are not statistically significant). ANOVA, analysis of variance; LD, lateral disc; PIA, posterior inferior attachment; PSA, posterior superior attachment; TMJ, temporomandibular joint; UTS, ultimate tensile strength.
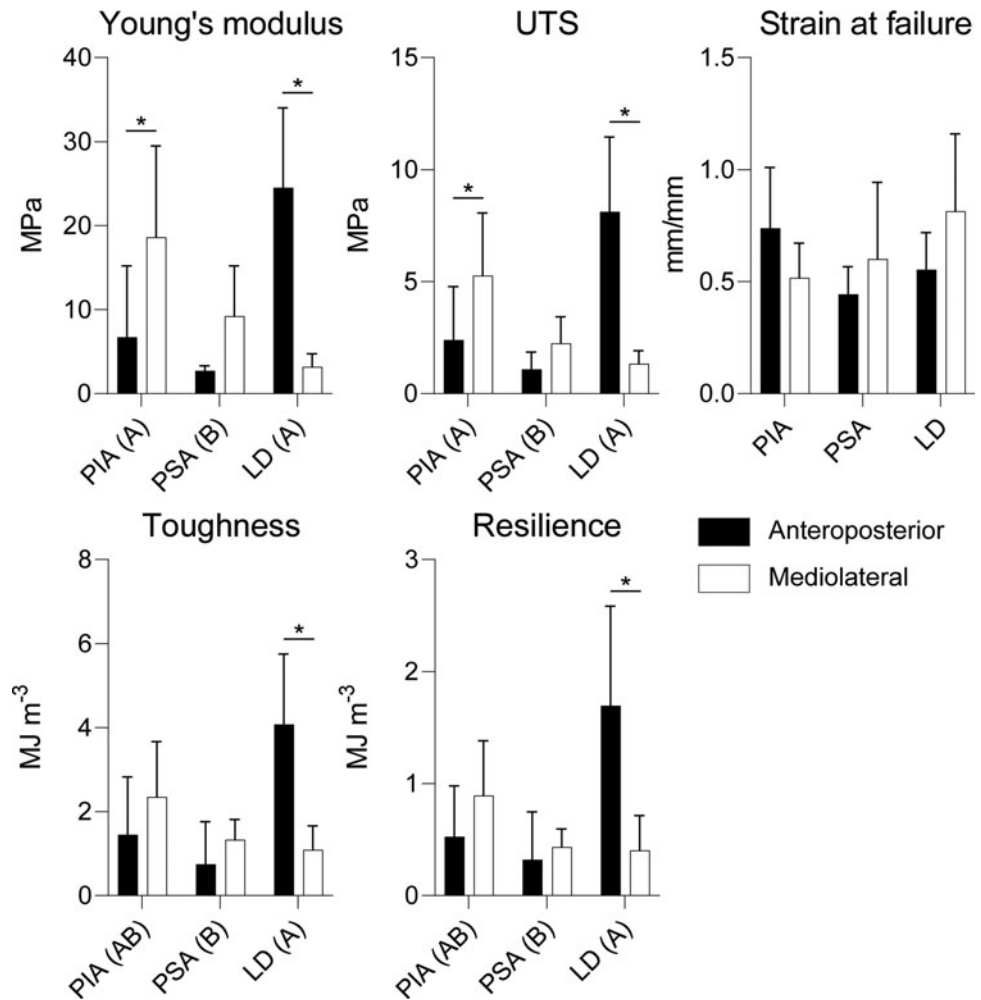
allow translation of the disc over the articular eminence during articulation. Most importantly, this study defines crucial design criteria and provides structure–function relationships for tissue-engineering and further understanding of the TMJ disc complex toward addressing the various TMJ pathologies afflicting millions.

The TMJ disc has been described as being highly anisotropic; it functions to allow stress absorption and dissipation during articulation.[35] Compressive stress applied by the condyle to the intermediate zone of the disc is transmitted to the anterior and posterior bands under tensile strains, similar to a trampoline's mesh.[30,36] This is accomplished by the anisotropic nature of the TMJ disc, being aligned in the AP direction in the intermediate zone, while the anterior and posterior bands are aligned in the ML direction, continuing circumferentially around the disc.[22,37] As expected, results from uniaxial tensile testing for the lateral disc showed significantly stiffer, stronger, tougher, and more resilient tissue in the AP direction compared with the ML direction, in agreement with previous literature.[22,37] However, when examining the PIA and PSA under uniaxial tension in this study, both attachments showed higher values in the ML direction compared with the AP direction, similar to that of the posterior band of the disc. For example, the PIA and PSA had 2.78 and 3.41 times higher ML stiffness values,

respectively, than those measured in the AP direction. When examining historical data from the attachments of juvenile farm pigs, the PSA exhibited similar anisotropy in terms of tensile properties, but the PIA was shown to be stiffer and stronger in the AP direction.[26] This difference may be due to age-, region-, or breed-related differences present in the posterior attachments. In future studies, it would be interesting to consider sampling from more medial or lateral regions of the posterior attachments to understand how structural differences among regions may relate to various functional differences. However, when examining AP stiffness in this study, the PIA still exhibited values 2.48 times higher than those of the PSA, which is consistent with prior literature that showed a 5.00 times higher stiffness.[26] In terms of resilience and toughness, PSA values were significantly lower than lateral disc values, with PIA values not being significantly different from either. Resilience and toughness are related to energy absorption and energy dissipation. Thus, these differences in resilience and toughness suggest different mechanical contributions of each region to the function of stress absorption and dissipation of the TMJ disc complex. This may, in part, be due to the presence of fat vacuoles (i.e., heterogeneity) in the PSA, affecting the mechanical properties. Regardless, based on mechanical data of posterior attachments, these data strongly indicate
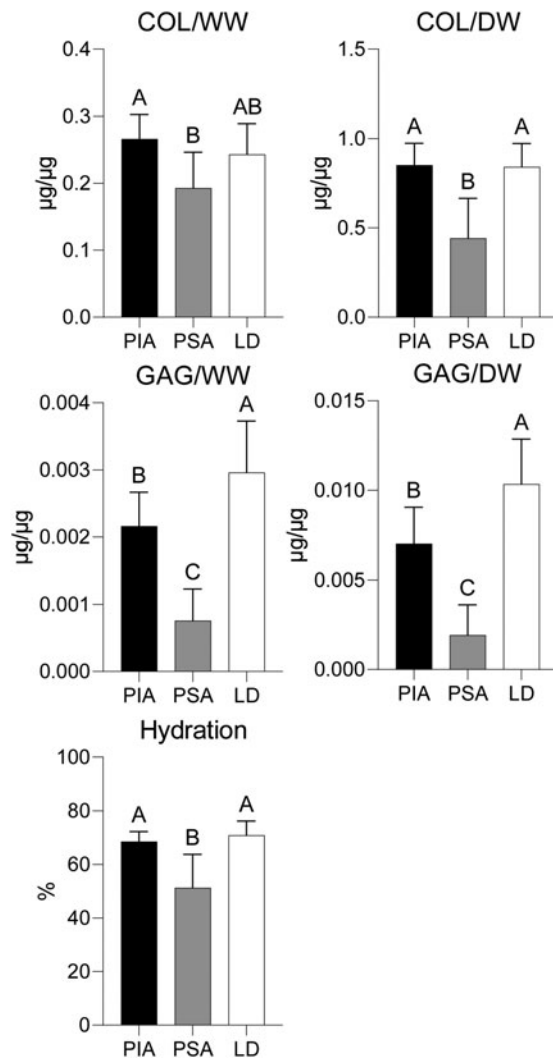
FIG. 5. Photometric biochemical testing outcomes of the TMJ disc complex. When examining both collagen per WW and collagen per DW, the PSA values were significantly lower than the PIA. GAG per WW and GAG per DW were significantly different among all groups, while tissue hydration was significantly higher in the lateral disc compared with the PSA. Statistics: one-way ANOVA, $p < 0.05$. Tukey's *post hoc* test among the locations is depicted with Latin letters above each bar through a connecting letters report (groups that share a letter are not statistically significant). ANOVA, analysis of variance; COL, collagen; DW, dry weight; GAG, glycosaminoglycan; LD, lateral disc; PIA, posterior inferior attachment; PSA, posterior superior attachment; TMJ, temporomandibular joint; WW, wet weight.

that the PIA and PSA play a crucial role in absorbing and dissipating stress during articulation, acting similarly to the springs of a trampoline.

There are also organizational and biochemical differences among the posterior attachments and the lateral disc. For example, it was found that the PIA and lateral disc have at least 1.91 times higher total collagen per DW than the PSA, which correlated with the PIA and lateral disc being stiffer and stronger than the PSA. This finding is similar to prior studies that showed the PSA had lower collagen content than the PIA and lateral disc.[38] As shown in the H&E

staining, this discrepancy in collagen content among the TMJ disc complex regions is likely due to the large degree of heterogeneity present in the PSA. Furthermore, crosslinking outcomes of the different regions further supported the tensile data. When examining the collagen alignment under polarized light microscopy, it was shown that the lateral disc is highly aligned in the AP direction. Contrastingly, the PIA and PSA were more aligned in the ML direction, but to a lesser extent when compared with the lateral disc. Together with the mechanical outcomes, these results establish gold-standard design criteria for tissue-engineering of a biomimetic TMJ disc complex.

The posterior attachments have been previously described as an extension of the TMJ disc, exhibiting a seamless transition from disc to attachment.[38] Histologically, the fibrous areas of the three tissues appeared strikingly similar in collagen and GAG contents, as shown by staining intensities of picrosirius red and safranin O. Additionally, prior literature has described elastin to compose between 3% and 7% per DW of the TMJ disc and it has been speculated to contribute to tissue recovery after deformation.[39] While not investigated here, prior work reported that the PIA, PSA, and lateral disc of juvenile porcine TMJ disc complexes show similar staining intensity for elastin as well.[38] The largest differences here appeared in tissue heterogeneity; a gradual transition from a fibrous to fibro-fatty tissue was seen when moving from the lateral disc to the posterior attachments, as shown by an increase in the amount of fat vacuoles present. This transition was also observed in the GAG content; the lateral disc exhibited the most GAG per DW, which was 1.48 and 5.39 times higher than the PIA and PSA, respectively. Additionally, the GAG contents of all tissues examined here were still far less than tissues that function mainly under compression, such as hyaline articular cartilage of the knee.[40] This may be associated with the primary role of the TMJ disc complex to undergo tensile stresses,[4] rather than the compressive stresses that are commonly associated with hyaline articular cartilage. It should also be noted that there may be some differences in the porcine and human posterior attachments, such as the degree of fat presence[26,41] and tissue exposure due to a less prominent postglenoid process.[42] These differences should be further investigated as the Yucatan minipig is established as modeling human TMJ conditions. Despite these differences, it should be mentioned that the Yucatan minipig exhibits substantial similarities to the human TMJ, for example, in terms of size, anatomy, function, diet, and chewing patterns.[22,27] These findings suggest that the three porcine tissues examined here function similarly under tension while transitioning from a fibrocartilaginous to fibro-fatty composition.

The nature of the PIA and PSA has been previously described as ligamentous.[3,38] In ligaments, the degree of collagen crosslinking is typically higher than those of fibrocartilaginous tissues, such as the knee meniscus or TMJ disc. For example, in a study examining the degree of crosslinking in various tissues of the knee, it was found that the cranial and caudal ligaments had a significantly higher degree of collagen crosslinking than the fibrocartilaginous meniscus.[43] When examining the degree of collagen crosslinking, both the PIA and PSA exhibited higher values than the fibrocartilaginous lateral disc. Thus, the crosslinking data showed that the function of PIA and PSA
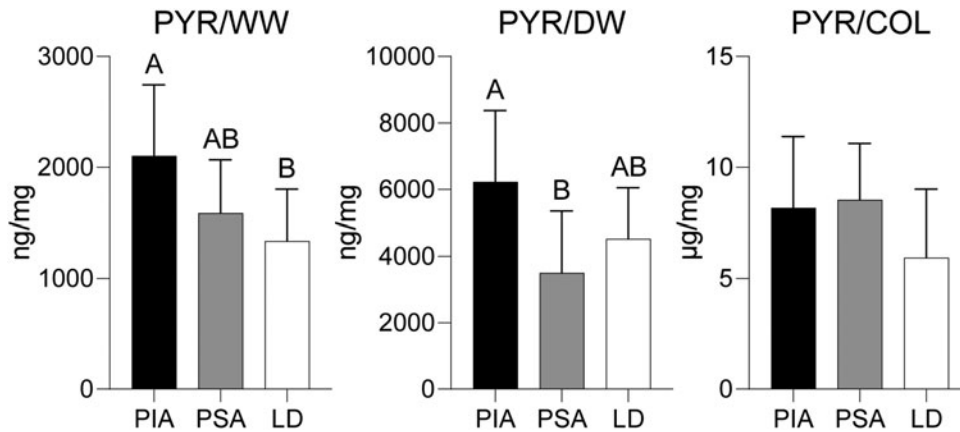
FIG. 6. Crosslinking mass spectrometry outcomes of the TMJ disc complex. When examining PYR per WW and PYR per DW, the PIA had higher values than those of the PSA. The degree of collagen crosslinking trended higher in the posterior attachments when compared with the lateral disc. Statistics: one-way ANOVA, $p < 0.05$. Tukey's *post hoc* test among the locations is depicted with Latin letters above each bar through a connecting letters report (groups that share a letter are not statistically significant). ANOVA, analysis of variance; COL, collagen; DW, dry weight; LD, lateral disc; PIA, posterior inferior attachment; PSA, posterior superior attachment; PYR, pyridinoline; TMJ, temporomandibular joint; WW, wet weight.

may be similar to ligaments, which operate under high tensile strains. With regard to mechanical properties, despite having lower degrees of crosslinking, the fibrocartilaginous meniscus displayed higher stiffness and strength values compared with the cranial and caudal ligaments of the knee.[43] Analogously, the fibrocartilaginous lateral disc exhibited the highest stiffness and strength values here as well, compared with the PIA and PSA. Whereas the crosslink and mechanical data suggest that the PIA and PSA are similar to ligaments, both of these tissues also display marked differences from ligaments. For example, while the PIA and PSA were found to be anisotropic, the degree of anisotropy is not as high as that of ligaments; it is known that ligaments are typically highly aligned in one direction.[44] Additionally, the heterogeneity found within the matrices of the PIA and PSA, mainly the presence of fat vacuoles, is dissimilar to the homogeneous composition of ligaments. Despite these differences, the ligament-like function of the posterior attachments is still crucial to the overall function of the TMJ disc complex. Consistent with the properties described above, the stiffer PIA may play a role in securing the disc to the condyle during articulation, while the softer PSA could allow translation of the disc over the articular eminence.

This study established design criteria and informed structure–function relationships for the TMJ disc complex. Toward tissue-engineering a functional biomimetic implant exactly like the native TMJ disc complex, engineers may use the structural, mechanical, biochemical, and crosslinks data presented here as design criteria. However, reaching complete biomimicry may not be necessary in all cases. For example, in a study examining healing of partial-thickness defects in the Yucatan minipig TMJ disc, implants that reached 42% of native tissue mechanical and biochemical properties (measured by a functionality index that weighs various outcome measures equally and normalizes them to native tissue) were adequate to induce robust and complete healing in 8 weeks.[28] Similarly, this may be the case for the posterior attachments, with implants needing to only reach a certain level of biomimicry to induce healing. Alternatively, tissue engineers may also prioritize certain design criteria

over others. For example, in the case of the TMJ disc complex, Young's modulus, UTS, and total collagen may be the primary design criteria, because the tissues function mainly under tensile strains, and collagen is most abundant in these tissues. In terms of structure–function relationships, there were no strong correlations among the biochemical and crosslink contents and the mechanical properties. Weak correlations between total collagen and crosslink contents and some tensile outcomes in the AP direction were found. Importantly, the field also needs to fully characterize the human TMJ disc complex to establish design criteria and compare structure–function relationships with the Yucatan minipig model. Unfortunately, there is not yet a comprehensive study doing so in the literature. By developing design criteria and investigating structure–function relationships, the TMJ field will rapidly move toward generating adequate implants for investigating healing in various defect models.

The mechanical and biochemical results of this study suggest that the posterior attachments operate under two functions: (1) both attachments act to distribute the compressive stresses applied during articulation by converting them into tensile stresses, supporting this function in the disc; and (2) the PIA acts to secure the disc to the condyle during articulation, while the PSA allows smooth translation over the articular eminence. For distribution of compressive stresses applied by the condyle, the TMJ disc complex acts together as one unit toward stress distribution during articulation. This was shown by the extension of ML alignment into the posterior attachments, which is present in the posterior band of the TMJ disc.[22] In terms of functioning to hold the disc in the proper position during articulation, within the TMJ disc complex, the PSA and PIA were shown to serve different functions. Specifically, in comparison with the PSA, the PIA demonstrated higher tensile properties, increased collagen content, and more PYR content, all indicating a more robust structure. Furthermore, both the PIA and PSA were found to be more heterogeneous, exhibiting fat vacuoles, and less fibrocartilaginous than the lateral disc as determined by the GAG content. These data support the

notion of a fibrocartilaginous to fibro-fatty spectrum upon which the tissues of the TMJ disc complex exist. Also, based on the literature,[38] all three regions exhibit similar elastin content. Thus, the fat vacuoles, collagen content, and crosslinking content may be greater contributors to differences among the three regions of the TMJ disc complex when compared to elastin. In addition, the posterior attachments have been previously described as ligamentous tissues.[3,38] However, the posterior attachments exhibit crucial differences from ligaments, such as lack of strong alignment and heterogeneity in the matrix content, but still play a ligament-like role during articulation. These properties support that, during articulation, the PIA may function to secure the disc to the condyle, while the PSA allows smooth translation of the disc–condyle unit over the articular eminence. Most importantly, this characterization study seeks to give tissue engineers gold-standard design criteria to aim for when engineering biomimetic implants for addressing pathologies of the TMJ disc complex, including anterior disc displacement and resulting lateral defects, toward relieving pain and improving function for the many patients with TMJ afflictions.

Authors' Contributions

R.P.D. and E.G.K. collected and analyzed the data. All authors designed the experiment, interpreted the results, drafted the article, critically edited the article, and approved the final version of the article.

Disclosure Statement

R.P.D., J.C.H., and K.A.A. are consultants for Cartilage Inc.

Funding Information

References

1. Zarb GA, Carlsson GE. Temporomandibular disorders: Osteoarthritis. J Orofac Pain 1999;13(4):295–306.
2. Alomar X, Medrano J, Cabratosa J, et al. Anatomy of the temporomandibular joint. Semin Ultrasound CT MR 2007; 28(3):170–183; doi: 10.1053/j.sult.2007.02.002
3. Scapino RP, Obrez A, Greising D. Organization and function of the collagen fiber system in the human temporomandibular joint disk and its attachments. Cells Tissues Organs 2006;182(3–4):201–225; doi: 10.1159/000093969
4. Donahue RP, Hu JC, Athanasiou KA. Remaining hurdles for tissue-engineering the temporomandibular joint disc. Trends Mol Med 2019;25(3):241–256; doi: 10.1016/j.molmed.2018.12.007
5. Johansson A, Unell L, Carlsson GE, et al. Gender difference in symptoms related to temporomandibular disorders in a population of 50-year-old subjects. J Orofac Pain 2003;17(1):29–35.
6. Macfarlane TV, Blinkhorn AS, Davies RM, et al. Orofacial pain in the community: prevalence and associated impact. Commun Dent Oral Epidemiol 2002;30(1):52–60; doi: 10.1034/j.1600-0528.2002.300108.x

7. Pow EH, Leung KC, McMillan AS. Prevalence of symptoms associated with temporomandibular disorders in Hong Kong Chinese. J Orofac Pain 2001;15(3):228–234.
8. Goulet JP, Lavigne GJ, Lund JP. Jaw pain prevalence among French-speaking Canadians in Quebec and related symptoms of temporomandibular disorders. J Dent Res 1995;74(11):1738–1744; doi: 10.1177/00220345950740110401
9. Solberg WK, Woo MW, Houston JB. Prevalence of mandibular dysfunction in young adults. J Am Dent Assoc 1979;98(1):25–34; doi: 10.14219/jada.archive.1979.0008
10. Farrar WB, McCarty WL, Jr. The TMJ dilemma. J Ala Dent Assoc 1979;63(1):19–26.
11. Tasaki MM, Westesson PL, Isberg AM, et al. Classification and prevalence of temporomandibular joint disk displacement in patients and symptom-free volunteers. Am J Orthod Dentofacial Orthop 1996;109(3):249–262; doi: 10.1016/s0889-5406(96)70148-8
12. Foucart JM, Carpentier P, Pajoni D, et al. MR of 732 TMJs: anterior, rotational, partial and sideways disc displacements. Eur J Radiol 1998;28(1):86–94; doi: 10.1016/s0720-048x(97)00102-2
13. Wilkes CH. Internal derangements of the temporomandibular joint. Pathological variations. Arch Otolaryngol Head Neck Surg 1989;115(4):469–477; doi: 10.1001/archotol.1989.01860280067019
14. Murray GM, Bhutada M, Peck CC, et al. The human lateral pterygoid muscle. Arch Oral Biol 2007;52(4):377–380; doi: 10.1016/j.archoralbio.2006.10.002
15. Katzberg RW, Westesson P-L. Diagnosis of the temporomandibular joint. W.B. Saunders: Philadelphia, PA; 1993.
16. Munoz-Guerra MF, Rodriguez-Campo FJ, Escorial Hernandez V, et al. Temporomandibular joint disc perforation: Long-term results after operative arthroscopy. J Oral Maxillofac Surg 2013;71(4):667–676; doi: 10.1016/j.joms.2012.12.013
17. Kuribayashi A, Okochi K, Kobayashi K, et al. MRI findings of temporomandibular joints with disk perforation. Oral Surg Oral Med Oral Pathol Oral Radiol Endod 2008; 106(3):419–425; doi: 10.1016/j.tripleo.2007.11.020
18. Liu XM, Zhang SY, Yang C, et al. Correlation between disc displacements and locations of disc perforation in the temporomandibular joint. Dentomaxillofac Radiol 2010; 39(3):149–156; doi: 10.1259/dmfr/72395946
19. Bielajew BJ, Donahue RP, Espinosa MG, et al. Knee orthopedics as a template for the temporomandibular joint. Cell Rep Med 2021;2(5):100241; doi: 10.1016/j.xcrm.2021.100241
20. Donahue RP, Gonzalez-Leon EA, Hu JC, et al. Considerations for translation of tissue engineered fibrocartilage from bench to bedside. J Biomech Eng 2018; doi: 10.1115/1.4042201
21. Murphy MK, MacBarb RF, Wong ME, et al. Temporomandibular disorders: A review of etiology, clinical management, and tissue engineering strategies. Int J Oral Maxillofac Implants 2013;28(6):e393–e414; doi: 10.11607/jomi.te20
22. Vapniarsky N, Aryaei A, Arzi B, et al. The Yucatan minipig temporomandibular joint disc structure-function relationships support its suitability for human comparative studies. Tissue Eng Part C Methods 2017;23(11):700–709; doi: 10.1089/ten.tec.2017.0149
23. Gutman S, Kim D, Tarafder S, et al. Regionally variant collagen alignment correlates with viscoelastic properties

of the disc of the human temporomandibular joint. Arch Oral Biol 2018;86:1–6; doi: 10.1016/j.archoralbio.2017.11.002

24. Allen KD, Athanasiou KA. Viscoelastic characterization of the porcine temporomandibular joint disc under unconfined compression. J Biomech 2006;39(2):312–322; doi: 10.1016/j.jbiomech.2004.11.012

25. Detamore MS, Athanasiou KA. Tensile properties of the porcine temporomandibular joint disc. J Biomech Eng 2003;125(4):558–565; doi: 10.1115/1.1589778

26. Murphy MK, Arzi B, Hu JC, et al. Tensile characterization of porcine temporomandibular joint disc attachments. J Dent Res 2013;92(8):753–758; doi: 10.1177/0022034513494817

27. Almarza AJ, Brown BN, Arzi B, et al. Preclinical animal models for temporomandibular joint tissue engineering. Tissue Eng Part B Rev 2018;24(3):171–178; doi: 10.1089/ten.TEB.2017.0341

28. Vapniarsky N, Huwe LW, Arzi B, et al. Tissue engineering toward temporomandibular joint disc regeneration. Sci Transl Med 2018;10(446):1–10; doi: 10.1126/scitranslmed.aaq1802

29. National Institutes of Health. Consideration of Sex as a Biological Variable in NIH-funded Research, 2015. Available from: https://orwh.od.nih.gov/sex-gender/nih-policy-sex-biological-variable [Last accessed: January 31, 2023].

30. Allen KD, Athanasiou KA. A surface-regional and freeze-thaw characterization of the porcine temporomandibular joint disc. Ann Biomed Eng 2005;33(7):951–962; doi: 10.1007/s10439-005-3872-6

31. Donahue RP, Nordberg RC, Bielajew BJ, et al. The effect of neonatal, juvenile, and adult donors on rejuvenated neocartilage functional properties. Tissue Eng Part A 2022;28(9–10): 383–393; doi: 10.1089/ten.TEA.2021.0167

32. Greiner C, Grainger S, Farrow S, et al. Robust quantitative assessment of collagen fibers with picrosirius red stain and linearly polarized light as demonstrated on atherosclerotic plaque samples. PLoS One 2021;16(3):e0248068; doi: 10.1371/journal.pone.0248068

33. Cissell DD, Link JM, Hu JC, et al. A modified hydroxyproline assay based on hydrochloric acid in ehrlich's solution accurately measures tissue collagen content. Tissue Eng Part C Methods 2017;23(4):243–250; doi: 10.1089/ten.tec.2017.0018

34. Bielajew BJ, Hu JC, Athanasiou KA. Methodology to quantify collagen subtypes and crosslinks: Application in minipig cartilages. Cartilage 2021;13(2_suppl):1742S–1754S; doi: 10.1177/19476035211060508

35. Sindelar BJ, Herring SW. Soft tissue mechanics of the temporomandibular joint. Cells Tissues Organs 2005;180(1):36–43; doi: 10.1159/000086197

36. Fazaeli S, Ghazanfari S, Everts V, et al. The contribution of collagen fibers to the mechanical compressive properties of the temporomandibular joint disc. Osteoarthritis Cartilage 2016;24(7):1292–1301; doi: 10.1016/j.joca.2016.01.138

37. Kalpakci KN, Willard VP, Wong ME, et al. An interspecies comparison of the temporomandibular joint disc. J Dent Res 2011;90(2):193–198; doi: 10.1177/0022034510381501

38. Willard VP, Arzi B, Athanasiou KA. The attachments of the temporomandibular joint disc: A biochemical and histological investigation. Arch Oral Biol 2012;57(6):599–606; doi: 10.1016/j.archoralbio.2011.10.004

39. Huwe LW, Hu JC. Structure and function of the TMJ disc and disc attachments. In: Specialty Imaging: Temporomandibular Joint. (Tamimi D, Hatcher D., eds.) 2017; pp. 50–53.

40. Athanasiou KA, Darling EM, DuRaine GD, et al. Articular Cartilage. CRC Press: Boca Raton, FL; 2017.

41. Rees LA. The structure and function of the mandibular joint. Br Dent, J 1954;96:125–133.

42. Herring SW, Decker JD, Liu ZJ, et al. Temporomandibular joint in miniature pigs: anatomy, cell replication, and relation to loading. Anat Rec 2002;266(3):152–166; doi: 10.1002/ar.10049

43. Eleswarapu SV, Responte DJ, Athanasiou KA. Tensile properties, collagen content, and crosslinks in connective tissues of the immature knee joint. PLoS One 2011;6(10):e26178; doi: 10.1371/journal.pone.0026178

44. Schmidt EC, Chin M, Aoyama JT, et al. Mechanical and microstructural properties of pediatric anterior cruciate ligaments and autograft tendons used for reconstruction. Orthop J Sports Med 2019;7(1):2325967118821667; doi: 10.1177/2325967118821667

Address correspondence to:
Kyriacos A. Athanasiou, PhD
Department of Biomedical Engineering
University of California, Irvine
3418 Engineering Hall
Irvine, CA 92697
USA

E-mail: Athanasiou@rics.edu